Standing Spin Waves as a Basis for the Control of Terahertz Spin Dynamics: Time Dependent Density Functional Theory Study

Paweł Buczek,* Arthur Ernst, and Leonid M. Sandratskii
Max Planck Institute of Microstructure Physics, Weinberg 2, 06120 Halle/S., Germany
(Received 4 May 2010; published 27 August 2010)

We report on the linear response density functional study of the magnetization dynamics in Co(100) film driven by a nonuniform magnetic field. At resonant frequencies in the terahertz range, the magnetic field excites standing spin waves of the system and the induced magnetization penetrates the whole volume of the film. The pattern of magnetization precession is strongly influenced by the spin-flip excitations of single electrons which lead to the Landau damping of the spin-wave modes. Our results pave the way for the precise control of terahertz magnetization dynamics in itinerant magnets.

DOI: 10.1103/PhysRevLett.105.097205 PACS numbers: 75.30.Ds, 75.40.Gb, 76.50.+g, 85.75.−d

The properties of excited states of magnetic materials and the interactions between different excitation types have become one of the central topics of the modern solid state research. Taking few examples, we first mention the experiments on subpicosecond demagnetization of laser irradiated ferromagnetic films [1,2], for which the channel for the ultrafast transfer of the angular momentum remains a matter of debate. Another example is the study of the lifetime of the image-potential states revealing its strong spin dependence explained by the spin-wave emission by spin-minority electrons [3]. Modern experiments, spin polarized electron energy loss spectroscopy [4], and inelastic scanning tunneling microscopy [5] allow us to measure the characteristics of spin waves in thin films providing the proof that even high energy magnon modes are well defined. The magnetic excitations can be employed as working medium in future spintronic devices [6]. For example, they have already been used to provide coupling between two spin-torque oscillators [7] or to construct logical gates [8]. Locally applied perturbation induces a significant magnetization response in distant parts of a device [9,10], which can be used for the interchip communication.

On the other hand, the parameter-free microscopic studies of the energies and life times of magnetic excitations are scarce. An adequate tool for such an analysis is the calculation of the dynamic magnetic spin susceptibility based on the linear response density functional theory [11]. Since the properties of collective magnetic modes (spin waves) and single electron spin flips (Stoner states) are sensitive to the electronic structure of a given material, a state-of-the-art *ab initio* technique is an important prerequisite to make a quantitative prediction. A proper description of the hybridization of these two types of excitations is necessary to describe correctly the Landau damping of magnons. Such computations are, however, very demanding both from the point of view of algorithmic complexity and computer resources and up to now have been performed only for simple bulk materials [12,13].

In the present Letter we report on the first parameter-free study of the pattern of precessing magnetization induced by a nonuniform external magnetic field applied to an ultrathin film. To achieve this aim we calculate dynamic magnetic spin susceptibility. We demonstrate that depending on the frequency and the shape of the field, the magnetic response in the film can vary from negligible to giant. The properties of the response are related to the calculated features of the magnetic eigenmodes which are standing spin waves in the case under study. We show that the Stoner states have an impact on the magnitude of the magnetization response and relative phases of precessing magnetic moments of different layers. The numerical scheme based on the Korringa-Kohn-Rostoker Green's function method applied previously to multiple-sublattice Heusler alloys [14] has been extended here to the study of thin films supported on a semi-infinite substrate or freestanding [15].

We begin with the study of spin dynamics in six monolayer thick freestanding Co(100) films. The presence of copper substrate alters in this case only weakly the properties of spin dynamics and will be addressed later. We consider the field applied to jth layer of the film

$$\mathbf{B}_j(t) = B_j(\cos\omega t, -\sin\omega t, 0). \quad (1)$$

The field is constant within the layer. The z axis is selected parallel to the sample magnetization. Even though in a real device applying field to a selected buried layer might not be an easy task, in theory such a gedanken experiment can be easily performed and provides additional insight into the physics of the problem. The frequency is considered positive for the clockwise oscillation of the field and negative in the opposite case. Although we consider the response to the magnetic field (typically encountered in ferromagnetic resonance experiments [16]) our results are relevant for many experiments where external perturbation excites magnetic states. The perturbation could be a beam of polarized electrons [17], a current [7,18], a laser field [1], or a decaying image-potential state electron [3]. The field (1) induces the precession of magnetic moments in all

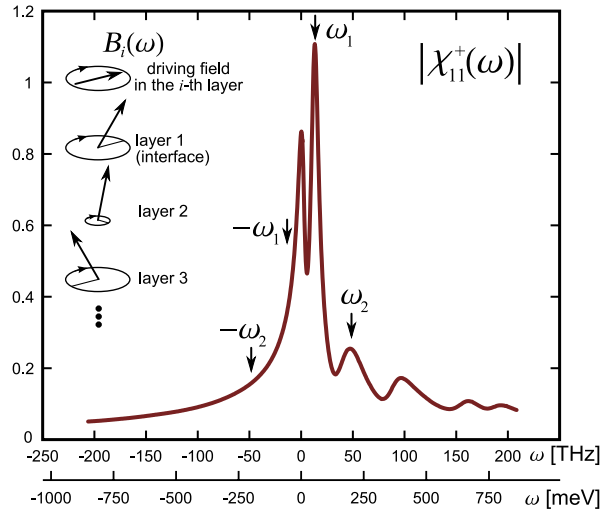

FIG. 1 (color online). The frequency dependence of the magnitude of the magnetization induced in the surface layer upon applying oscillating magnetic field in the same layer. The results are given in arbitrary units common for all figures in the paper. The inset shows the schematics of our theoretical experiment. 1 THz $\approx$ 4.135 meV.

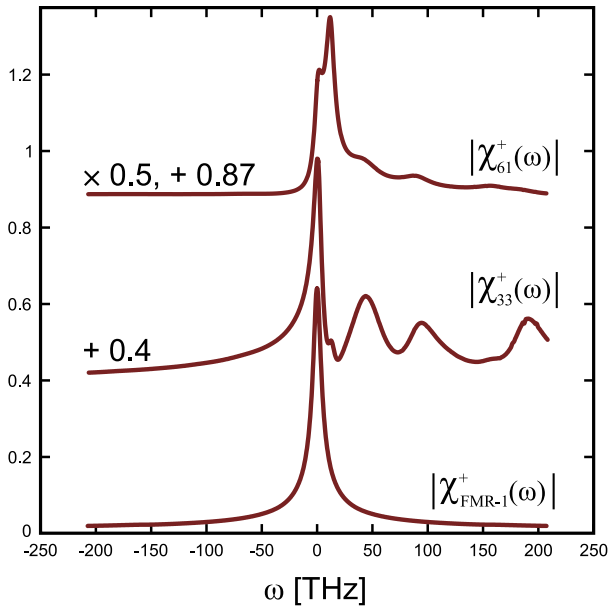

FIG. 2 (color online). The frequency dependence of the magnitude of the magnetization induced in different layers upon applying oscillating magnetic field in various layers. Two upper curves: the magnitude of magnetization induced in the 6th and 3rd layers upon application of the field in the 1st and the 3rd layers, respectively. The bottom curve presents the magnetization induced in the first layer by a field uniform in the *whole* film. The curves are shifted vertically for the sake of clarity.

layers [cf. the inset of Fig. 1], and the uniform component of induced magnetization in the ith layer is given by

$$\mathbf{m}_i(t) = m_i(\omega)(\cos\varphi, -\sin\varphi, 0) \tag{2}$$

where $\varphi \equiv \omega t + \phi_i(\omega)$ and m_i and ϕ_i are, respectively, layer-dependent amplitude and phase of the induced magnetization. The susceptibility $\chi^+_{ij}(\omega)$ determined in our linear response density functional theory calculations gives the relation between $\mathbf{m}_i$ and $\mathbf{B}_j$. The absolute value of the susceptibility reads

$$|\chi^+_{ij}(\omega)| = \frac{m_i(\omega)}{B_j}. \tag{3}$$

In Fig. 1 we present the calculated frequency dependence of $|\chi^+_{11}(\omega)|$, describing the magnetization of the surface layer induced by the field applied to the same layer. There is a series of six peaks appearing at positive frequencies. The heights and widths of the peaks differ strongly between each other. In Fig. 2 we plot a number of different magnetic responses. The response in the 6th layer to the field applied to the first layer, $|\chi^+_{61}|$, features the same peak positions as $|\chi^+_{11}|$ [Fig. 1]. In the low energy range, the heights of the peaks are comparable in both cases, whereas for high energies the peaks in $|\chi^+_{61}|$ are less pronounced. Applying the field to the 3rd layer and analyzing the response $|\chi^+_{33}|$ in the same layer, we again obtain the peaks at the same positions. There are, however, strong changes in the relative height of the peaks compared to $|\chi^+_{11}|$.

The common frequency positions of the peaks in all cases and the number of the peaks equal to the number of the magnetic layers suggest that the maxima of magnetic responses are determined by collective eigenmodes of the film. Another important feature of the magnetic response is its asymmetry with respect to the change of the sign of the frequency. The association of the peaks with the collective eigenmodes explains this property. Its origin is in the broken time-reversal symmetry in the ferromagnetic ground state. The fact that the peaks appear only for the positive frequencies reflects intrinsic chirality of the precessional eigenstates. Later, we will confirm the hypothesis by the direct calculation of magnetic excited states of the film.

To get a deeper insight into the nature of the peaks, we analyze the layer dependence of the susceptibility at the frequencies corresponding to the peak positions [Fig. 3]. We consider again the case of the field applied to the first layer and focus on the two well-defined resonances at $\omega_1 = 12.8$ THz (52.8 meV) and $\omega_2 = 46.4$ THz (192 meV) [cf. Fig. 1]. In the resonance ω_1, the large response is observed at both surfaces of the film, while the magnetization in the center precesses with visibly smaller amplitude; the magnetization profile is almost symmetric with respect to the center of the film. For $\omega = \omega_2$ the pattern is more complex. There are two minima corresponding to the layers directly adjacent to the surface layers with the fifth layer participating very weakly in the precession. The central symmetry is not present. For comparison, we show in Fig. 3 the layer dependence of induced transverse moments for frequencies opposite to ω_1 and ω_2. In the case of the counter-clockwise polarized field the induced magnetization does not penetrate into the film. The magnitude of the deviation decreases strongly and

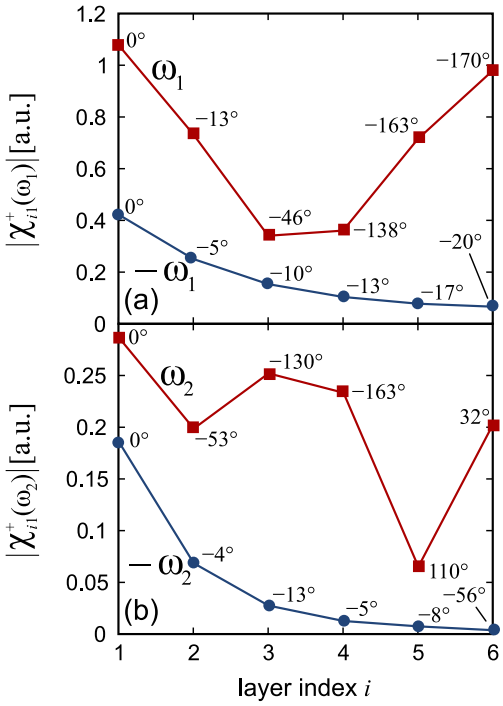

FIG. 3 (color online). Layer-resolved profile of induced magnetization upon applying oscillating magnetic field in the surface layer. Two resonant frequencies marked $\omega_{1,2}$ in Fig. 1 are considered together with their counterparts of opposite polarization ($-\omega_{1,2}$). The angles along the lines represent the relative phases of the moments in their precessional motion.

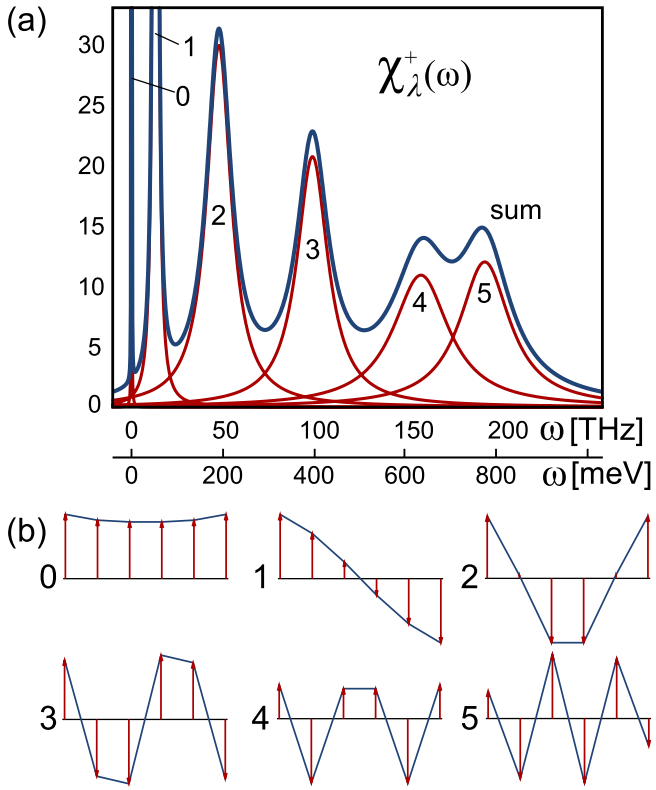

FIG. 4 (color online). Spectral power of spin excitations. (a) Eigenvalues $\chi^+_\lambda(\omega)$ of the loss matrix, atomic units. Six Lorentzian peaks can be distinguished. The envelope denotes the sum over all the eigenvalues. (b) Corresponding eigenvectors. The arrows present layer-resolved transverse components of the magnetization at a certain moment in time. With time, all moments precess about the z axis.

monotonically with increasing distance from the driven layer. The decay of the amplitude is stronger for larger frequency.

We turn now to the calculation of the excitation spectrum. Our calculational technique allows us to determine the precessional eigenmodes defined as the eigenstates of the *loss matrix* $\chi^+_{Lij}(\omega)$

$$2i\chi^+_{Lij}(\omega) = \chi^+_{ij}(\omega) - \chi^+_{ji}(\omega)^* \tag{4}$$

given by the imaginary part of the dynamic susceptibility. The fluctuation-dissipation theorem tells us that the eigenvalues of the loss matrix, $\chi^+_\lambda(\omega)$, are proportional to the energy absorption from the external field of shape $m^+_{\lambda i}(\omega)$, the latter quantity being the corresponding eigenvector. Index λ labels eigenvalues. A similar analysis has been performed in Refs. [14,19]. The frequency dependence of particular eigenvalues is of Lorentzian form [Fig. 4(a)]. The positions of the peaks maxima represent the spin-wave energies. They correspond perfectly to the peaks in the $|\chi^+_{ij}(\omega)|$ response functions. The widths of the peaks signify the finite lifetime of the spin waves. Qualitatively, the calculated spectra are in good correlation with those obtained by Costa *et al.* [20] within parametrized tight-binding treatment of the electron structure. The analysis of substantial quantitative differences is of limited value because of the strong dependence of the results of Costa *et al.* on the choice of the Coulomb parameters.

Figure 4(b) shows the corresponding eigenvectors determined at the resonant frequencies (peak maxima). Mode 0 (Goldstone mode) involves the uniform precession of moments. Since in our calculations we neglect the spin-orbit coupling, the state appears formally at exactly zero frequency [21]. In real systems the position of the lowest-energy peak is determined by the strength of the magnetic anisotropy and is usually in the GHz range. High energy eigenmodes appear between 10 and 200 THz and feature node(s) in the body of the film. The dynamics at these high frequencies is governed by the exchange interaction since, while precessing, the moments of different layers are not parallel to each other. They are the standing spin waves of the film. All the modes are characterized by large deviations of the magnetization at the surface of the film. This feature explains why all modes can be excited by the field applied to the surface layer.

The shape of mode 1 with the node in the center of the film corresponds closely to the precession pattern from Fig. 3(a). The similarity is much weaker in the case of mode 2 [cf. Fig. 3(b)]. We can understand the difference once we notice that the resonance at ω_1 is very high and narrow: eigenmode 1 clearly dominates the response at this

frequency. The resonance of mode 2 is much less sharp which results in the substantial influence of nonresonant contributions in the layers close to the driving (surface) layer. We still obtain the characteristic double minimum pattern of the second eigenmode [compare Figs. 4(b) and 3(b)]; however, the response minimum in the second layer is less pronounced than in the 5th layer, distant from the driving one.

The mode broadening and overlap [Fig. 4(a)] is a consequence of the Landau damping. The latter has another, more subtle result, pertaining to the phases ϕ_j of the magnetization precession. In the case of undamped spin waves, the moments would be either parallel or antiparallel to each other while precessing upon the external driving. When the Stoner excitations are taken into account, the simple phase relationship is lost and the magnetic configurations become non-coplanar. To illustrate this property, we give in Fig. 3 the relative phases of atomic moments in their precessional motion for the cases considered in the figure. The phase properties are crucial for devices based on spin-wave interference [8].

The full width at the half maximum of peak 1 is around 1.26 THz. This means that after the external driving is switched off, the amplitude of the precession decreases to $e^{-1} \approx 0.37$ of its initial value after about 1.59 ps which corresponds to slightly more than three precessional periods. This time correlates nicely with time scale of the attenuation attributed to Stoner excitations and observed experimentally [1]. For comparison, mode 5 features the shortest lifetime of 55 fs, making only 1.4 revolutions during this time. This indicates that the Landau damping is a very efficient attenuation mechanism for the magnetization dynamics in metallic magnets at terahertz frequencies.

The calculations and analysis reported in this Letter provide a tool for the theoretical design of systems with desired magnetic dynamics. For instance, the magnetic field applied at the surface of the film causes, at certain frequencies, significant magnetization response at the opposite film interface [curve $|\chi^{+}_{61}(\omega)|$ in Fig. 2]. The effect could be useful when considering communication between distant parts of a device. If we applied the driving field at the third layer, the response at ω_1 would be small because mode 1 features a node there, whereas the response at ω_2 does not change compared to $|\chi^{+}_{11}(\omega)|$. If a uniform field were applied in the whole film only the uniform mode would be excited, cf. curve $|\chi^{+}_{\mathrm{FMR}-1}(\omega)|$ in Fig. 2. This uniform precession of magnetization is typically obtained in the ferromagnetic resonance experiments.

Finally, we comment on the impact the substrate has on the picture of spin dynamics presented above. The appearance of the substrate breaks the central symmetry of the film and the modes of the supported film are not any more either symmetric or antisymmetric with respect to the film's mirror plane. Additionally, a nonmagnetic metallic substrate introduces the continuum of low energy Stoner states to the system [20], which is a consequence of vanishing exchange splitting in the substrate. This, in general, enhances Landau damping, resulting in an increased width of spin-wave peaks. However, the damping enhancement due to substrate is very sensitive to the details of the hybridization between the electron states of the film and substrate. In the case of Co/Cu(100) our calculations (not presented here) show that the influence of the substrate is weak. In other systems the presence of substrate might lead to strong changes in the dynamic magnetic properties of the film [see, e.g., Fe/W(110) [22]].

In summary, we have presented an *ab initio* theory of externally driven magnetization dynamics in an ultrathin magnetic film. The key features of the complex patterns of induced magnetization precession can be interpreted in terms of the properties of the standing spin waves hybridizing with the continuum of Stoner excitations. The magnetization dynamics at terahertz frequencies is dominated by the exchange interaction and strongly influenced by the Landau damping.

We thank Z. Szotek for critical remarks on the manuscript.

*Corresponding author: pbuczek@mpi-halle.mpg.de

[1] A. Scholl *et al.*, Phys. Rev. Lett. **79**, 5146 (1997).
[2] B. Koopmans *et al.*, Nature Mater. **9**, 259 (2010).
[3] A. B. Schmidt *et al.*, Phys. Rev. Lett. **95**, 107402 (2005).
[4] Y. Zhang *et al.*, Phys. Rev. B **81**, 094438 (2010).
[5] T. Balashov *et al.*, Phys. Rev. B **78**, 174404 (2008).
[6] S. Neusser and D. Grundler, Adv. Mater. **21**, 2927 (2009).
[7] S. Kaka *et al.*, Nature (London) **437**, 389 (2005).
[8] T. Schneider *et al.*, Appl. Phys. Lett. **92**, 022505 (2008).
[9] Y. Kajiwara *et al.*, Nature (London) **464**, 262 (2010).
[10] A. T. Costa *et al.*, Phys. Rev. B **78**, 054439 (2008).
[11] E. K. U. Gross and W. Kohn, Phys. Rev. Lett. **55**, 2850 (1985).
[12] S. Y. Savrasov, Phys. Rev. Lett. **81**, 2570 (1998).
[13] E. Şaşioğlu *et al.*, Phys. Rev. B **81**, 054434 (2010).
[14] P. Buczek *et al.*, Phys. Rev. Lett. **102**, 247206 (2009).
[15] P. A. Buczek, Ph.D. thesis, Martin Luther Universität Halle-Wittenberg, 2009, http://digital.bibliothek.uni-halle.de/ulbhalhs/urn/urn:nbn:de:gbv:3:4-552.
[16] R. Urban, G. Woltersdorf, and B. Heinrich, Phys. Rev. Lett. **87**, 217204 (2001).
[17] R. Vollmer *et al.*, Phys. Rev. Lett. **91**, 147201 (2003).
[18] T. Balashov *et al.*, Phys. Rev. Lett. **97**, 187201 (2006).
[19] A. T. Costa, Jr., R. B. Muniz, and D. L. Mills, Phys. Rev. B **74**, 214403 (2006).
[20] A. T. Costa, Jr., R. B. Muniz, and D. L. Mills, Phys. Rev. B **69**, 064413 (2004); **70**, 054406 (2004).
[21] Due to imperfect numerical convergence, the energy of the Goldstone mode is not exactly zero and assumes the value of 2.8 meV in our case. For the sake of graphical presentation all peaks have been broadened by 5 meV.
[22] P. Buczek *et al.*, J. Magn. Magn. Mater. **322**, 1396 (2010).